Application of a new friction model in Circular Cup Drawing

Ravindra K. Saxena* and Anuj Sharma

Sant Longowal Institute of Engineering and Technology, Sangrur-148106 PB
*rksaxena04@yahoo.com

Abstract

In deep drawing operation, friction plays an important role. Friction also influences the stresses and strains in the work-piece material and, hence, the quality of the product. In sheet metal forming simulations, the Coulomb' friction model is often used. The friction coefficient is dependent on contact pressure and/or deformation of the sheet material. When two surfaces come in contact, the surface texture of a material changes due to the combination of normal loading and stretching. A recently proposed friction model based on the surface changes on the micro-scale is incorporated into an in-house FE deep drawing code to find its effect. The results show a realistic distribution of the coefficient of friction depending on the local process conditions.

Keywords: *Friction modeling, flattening mechanisms, real contact area, ploughing, adhesion.*

1. Introduction

Sheet metal forming processes like deep drawing, stretching, bending, etc. are widely used. If the cup depth is more than half the diameter of the drawn cup, the process is called deep drawing. In this process, the sheet metal is pushed through the die, which possesses the shape of the product to be drawn. The schematic of the deep drawing process is shown in Fig. 1 [Saxena 2009].

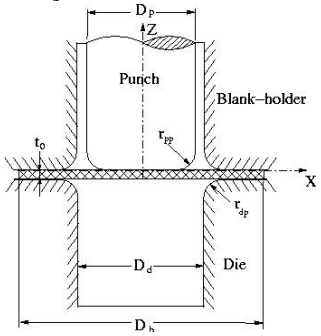

Figure 1: Schematic of Circular Cup Drawing

Deep drawing is effectively used for ductile metals, such as aluminum, brass, copper, and steel. Due to pre-processing, the sheet material has a specific roughness value which has an important influence on the deep drawing process. In deep drawing, friction originates from sliding contact between the tool and the sheet. In metal forming processes, friction affects the punch load, clamping forces, stresses, strain distribution, material flow, energy consumption and surface texture of the products. Many times, the formability of sheet metal depends on the friction at the tooling/work-piece interface in addition to its material properties. The friction in punch-sheet interface must be sufficiently high to ensure that the sheet follows the movement of the punch. The friction in the die-sheet and blankholder-sheet interface must not be too high, because a high friction leads to higher punch forces, resulting in fracture [Altan and Tekkaya 2012]. It is observed that the coefficient of friction does not remain constant throughout the contact surface for lubricated contacts due to varied internal and environmental conditions at contact.

Various friction models have been proposed in literature. Few of the popular models viz. Coulomb and Shear friction model [Karman 1925, Orowan 1946], Bowden and Tabor Model [1967], Dahl model [1968], General friction model [Wanheim et al. 1974, 1975], LuGre model [Canudas et al. 1995], Torrance et al. Friction Model [1997], Absolute Constant friction stress model [Tan et al. 1998], Empirical friction model [Tan 1999], and Levanov's Friction Model [Cora 2004] are used in different metal forming processes.

2. Literature Review

Challen & Oxley [1979] developed a model which takes the combined effect of ploughing and adhesion on the coefficient of friction. They performed a slip-line analysis on the deformation of a soft flat material by a hard wedge-shaped asperity. Wilson [1988] developed a separate friction model which treated independently the effect of adhesion and ploughing for calculating the coefficient of friction in metal forming. Yang et al. [1990] used the coulomb friction model incorporating relative displacement. Tan [2002] has examined five different models to analyze the upsetting of Al 6082 cylindrical test pieces viz. Coulomb friction model, shear friction model, general friction model, constant friction model and empirical friction model. Wang and Pelinescu [2003] used a Coulomb friction model to analyze the contact forces and connection flexibility between work-piece and fixture. Liu et al. [1985] and Ghosh et al. [2004] used a constant friction factor model in the study of the cold rolling process. Hol et al. [2012] developed a friction model which accounts for the change of the surface texture on the micro-scale and its influence on the friction behavior on the macro-scale.

The value of the coefficient of friction is dependent upon the surface asperities and stretching of the asperities. This phenomenon depends upon the

flattening mechanism viz. normal loading and strain condition of the deforming material. A friction model for the determination of the coefficient of friction incorporating the flattening mechanism at the localized region is proposed [Hol et al. 2012]. It is applied in the forging and rolling processes. In the present work, this friction model is incorporated to find its effect on cup drawing process. Following existing models have been used to describe the mechanisms of this variable friction coefficient:

- The flattening behavior of asperities due to normal loading; the contact model of Westeneng [2001].
- The flattening behavior of asperities due to straining; the strain model of Westeneng [2001].
- The influence of ploughing and adhesion on the coefficient of friction; Challen & Oxley [1979] model for multiple asperities.

2.1 Assumptions for friction model

The primary assumptions for calculating the friction coefficient [Hol et al. 2012] are as follows:

i. Material is ideal plastic and only plastic deformation of asperities is assumed without work hardening effects.
ii. Effect of temperature is neglected.
iii. Tool is rigid and harder than the work-piece.
iv. Surface asperities describing the roughness are assumed to be in the form of Gaussian distribution.
v. Boundary lubrication is considered between the tool and work-piece.
vi. Flattening due to sliding has been neglected.
vii. Soft and rough work-piece deforms in the normal and in the tangential direction both.

Friction models encompassing micro-mechanisms are generally difficult to be used in large-scale FE simulations. Therefore, translation technique is used to translate microscopic contact behavior to macroscopic contact behavior [Hol et al. 2012]. Using stochastic methods, rough surfaces are described on the micro-scale by their statistical parameters (mean radius of asperities, asperity density and the surface height distribution). Statistical parameters are used assuming the isotropic surface texture for the work-piece and tool material [Westeneng 2001].

2.2 Characterization of rough surfaces

A discrete surface height distribution of the tool and work-piece material is required from surface profiles (Fig. 2). For the ease of integrating the discrete distribution, it is approximated as a continuous function. Various methods exist to describe discrete signals by continuous functions. In the present work, it is assumed to follow Gauss distribution function because the surface height distribution is symmetric and approximates a normal distribution function:

$$\varphi(z) = \frac{1}{\sqrt{2\pi}} \exp\left(-\frac{z^2}{2}\right) \qquad (1)$$

2.3. Flattening mechanisms

Two flattening mechanisms have been implemented in the friction model to calculate the real area of contact of the work-piece viz. *flattening due to normal loading and flattening due to stretching.*

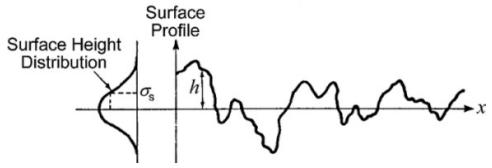

Figure 2: Representation of surface profile and surface height distribution [Westeneng 2001]

Westeneng [2001] assumed the tool as rigid and perfectly flat, which indents into a soft and rough work-piece material. Westeneng [2001] modeled the asperities of the rough surface by bars which can represent arbitrarily shaped asperities (Fig. 3). Westeneng [2001] introduced three stochastic variables as in Fig. 3 viz. the normalized surface height distribution function of the asperities of the rough surface $\varphi(z)$, the uniform rise of the non-contacting surface U (based on volume conservation) and the separation between the tool surface and the mean plane of the asperities of the rough surface d.

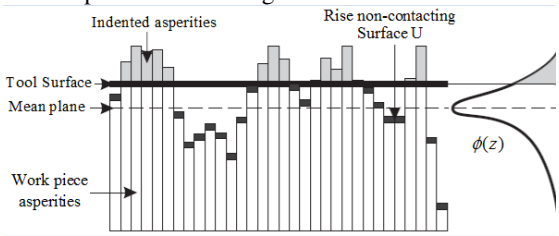

Figure 3: Indentation of soft rough surface by a smooth hard surface [Hol et al. 2012]

Flattening due to normal loading

The asperities of the sheet material deform under the applied normal load of the tool. For the analysis, the contact between a flat hard smooth tool surface and a soft rough sheet metal surface is assumed without sliding and bulk deformation. Ideal plastic deformation of asperities is assumed without work-hardening effects. To account for energy conservation the amount of external energy is assumed to be equal to the internal energy of deformation. The amount of external energy is described by the energy needed to indent contacting asperities. The internal energy is described by the energy absorbed by the indented asperities and the energy required for lifting up the non-contacting asperities. Further, a distinction is made between asperities in contact with the indenter, asperities which will come into contact due to the rise of asperities and asperities which will not come into contact with the indenter.

The amount of flattening 'd' of contacting asperities and the rise of non-contacting asperities U due to normal loading is calculated by solving Eq. (2) and Eq. (3) simultaneously [Hol et al. 2012]. The equations are presented based upon asperity deformation as:

$$\xi\left(1+\eta\chi\int_d^\infty \varphi(z)\,dz\right) - \frac{P_{nom}}{H} = 0 \qquad (2)$$

$$\int_{d-U}^{\infty}(z-d+U)\varphi(z)\,dz-U=0 \quad (3)$$

where, P_{nom} is the nominal pressure and H is the hardness of sheet asperities. These are two equations with unknowns d and U. The above sets of equations are solved for fraction of real contact area α, d and U by using the second order Newton-Raphson scheme.

Flattening due to stretching

The asperities of the sheet material also deform due to the stretching deformation of the material due to tangential load of the sliding contact. Westeneng [2001] derived an analytical contact model to describe the influence of strain on deforming, arbitrary shaped asperities. It is assumed that the effective hardness of asperities reduces under deformation. As a result, more flattening of contacting asperities occurs. The outcome of the ideal-plastic load model, for normal loading, is used as an input. Similar to the normal loading model, the stretching model considers contact between a flat hard surface and a soft rough surface. Only plastic material behavior is assumed without work hardening effects.

As a starting point, a single asperity on the soft surface is in contact with the tool. A fraction of real contact area of this asperity $\bar{\alpha}_s$ is defined. The change in $\bar{\alpha}_s$ as a function of the nominal strain ε, which for infinitesimally small changes of ε is defined as $d\overline{\alpha_s}/d\varepsilon$. It is assumed that the fraction of the real contact area for one asperity $\bar{\alpha}_s$ equals the total fraction of contact area α_s. Therefore, the stochastic form of the real contact area can be used to solve the differential equation

$$\frac{d\overline{\alpha_s}}{d\varepsilon}=\frac{l}{E}\varphi(d_s-U_s) \quad (4)$$

where, l is the mean half asperity spacing and E is the non-dimensional strain rate [30]. To calculate the change of α_s, the value of U_S and d_S is solved simultaneously while ε is incrementally increased. The differential equation in Eq. (4) is solved by applying the Euler Method [Jain et al. 2003].

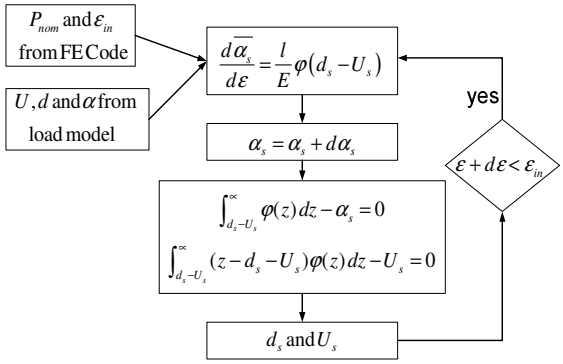

Figure 4: Flow chart for stretching model

Based on volume conservation, the equation:

$$\int_{d_s-U_s}^{\infty}\varphi(z)\,dz-\alpha_s=0 \quad (5)$$

and based on the definition of the fraction of real contact area, the equation:

$$\int_{d_s-U_s}^{\infty}(z-d_s-U_s)\varphi(z)\,dz-U_s=0 \quad (6)$$

are solved simultaneously using second order Newton-Raphson. Figure 6 shows the flow chart for calculating these coefficients for stretching model.

The model of Challen & Oxley [1979] has been used to calculate the coefficient of friction between a hard asperity and a soft flat surface. They performed a slip-line field analysis to describe contact conditions of wedged-shaped asperities. The model incorporates the combined effect of ploughing and adhesion between contacting surfaces.

The friction force acting on one asperity $F_{W_{asp}}$ is described by:

$$F_{W_{asp}}=\mu_{asp}F_{N_{asp}} \quad (5)$$

$F_{N_{asp}}$ represents the normal load on one asperity. A relation between the normal load $F_{N_{asp}}$ and the indentation ω is defined as [Hol et al. 2012]:

$$F_{N_{asp}}=\sqrt{2\omega\beta_t-\omega^2}\,bH \quad (6)$$

where, β_t is the radius of tool asperity, ω represents amount of indentation, b is the unit width of rough surface for a plane strain assumption and H is the hardness of the work surface.

Westeneng [2001] extended the model of Challen & Oxley [1979] to describe friction conditions between a flat work-piece material and multiple tool asperities. Total friction force is calculated as [Hol et al. 2012]:

$$F_W=\alpha_S A_{nom}\rho_t\int_{\delta}^{s\max}F_{W_{asp}}\varphi_t(s)\,ds \quad (7)$$

where, s denotes the asperity heights of tool surface, ρ_t denotes the asperity density of tool surface, σ_s denotes the deviation from the mean value of asperity heights and $F_{W_{asp}}$ the friction force occurring at a single asperity.

The coefficient of friction is calculated by

$$\mu=\frac{F_W}{F_N} \quad (8)$$

The friction model has been implemented into the in-house FE deep drawing code on MATLAB. The friction model is called independently for every node in contact on the die/blankholder surface during FE simulation. If a node is in contact, the nominal contact pressure and strain in the bulk material is called from the finite element code.

2.4. Formulation for Deep Drawing Simulation

Updated Lagrangian formulation is employed to develop the incremental finite element equations using eight-noded brick elements. Incremental logarithmic strain measure is used. The incremental stress is made objective by evaluating it in a frame rotating with the material particle. The material is assumed to be elasto-plastic strain hardening yielding according to the von-Mises yield criterion. The strain hardening behavior is modeled by a power law. Body forces are neglected and

due to small accelerations inertial forces are not included. Modified Newton–Raphson iterative technique is used to solve the non-linear incremental finite element equations [Saxena 2009].

3. Results and Discussion

Now, the model is applied to find out the effect of variable friction coefficient on deep drawing characteristics.

3.1. Validation

Sheet material DC 04 low carbon steel is used for the FE simulation with blank radius 79.38 mm (Table 1). Total blankholder force used is 22 kN for 1.6 mm plate thickness. Two sets of simulations have been performed in order to quantify the individual contributions of the two flattening mechanisms. The first set of simulation accounts for the influence of normal loading on the coefficient of friction and the second set of simulation use both flattening models to determine the coefficient of friction.

Table 1: Mechanical Properties for sheet Metal

Material parameter	Value
Elastic modulus	210 GPa
Poisson's ratio	0.3
Yield Strength	150 MPa
Hardening coefficient	500 MPa
Hardening exponent	0.2
Initial strain	0.00243

The surface properties of the work-piece are given in Table 4.2.

Table 4.2: Geometrical Properties for sheet Metal surface

Material parameter	Value
Work-piece hardness	1400 MPa
Persistence parameter(η)	1
Density of work-piece asperities	5000 mm^{-2}
Radius of tool asperity	0.002 mm
Roughness distribution	Standard distribution

For comparison purpose, the distribution of friction coefficient at a punch displacement of 25 mm is plotted. For the first set i.e. with normal loading, the friction coefficient varies from 0.12 to 0.142 throughout the contact region of the sheet material. The maximum value of friction coefficient observed just before the die profile radius region, Fig. 5. The grey color shows the zero value of friction coefficient.

For the second set i.e. with combined normal loading and stretching of the surface asperities, the friction coefficient varies from 0.12 to 0.22 (Fig. 6). All the process variables remain the same. The friction coefficient is higher for the second set of simulation. This increase is due to increase in real area of contact after the inclusion of stretching phenomenon.

The range of friction coefficient is in compliance to Hol et al. [2012] for the similar set of process varables. Hol et al. [2012] have used a cross shaped geometrical parameters whereas in the present work the simulation is perofrmed for circular cup drawing. It is observed that the predicted values of the coefficient of friction at different zones of the deformation are reasonable.

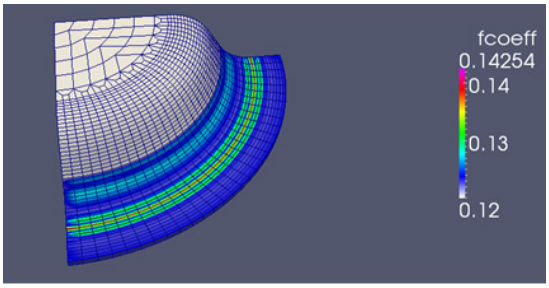

Figure 5: Development of coefficient of friction for normal loading

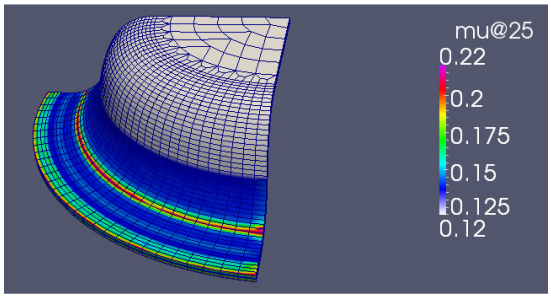

Figure 6: Development of coefficient of friction for normal loading + stretching

3.2. Parametric Study

A parametric study is performed for getting the effect of friction model with normal loading and with a combined effect of normal loading and stretching on different process variables for circular cup drawing.

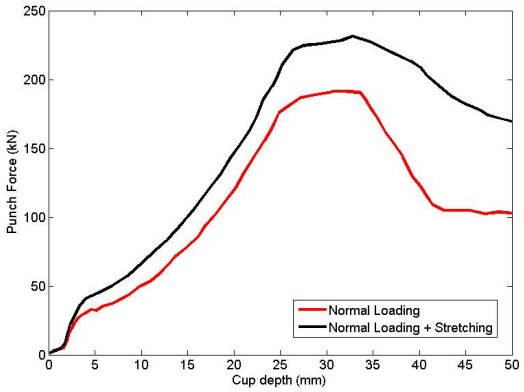

Figure 7: Relationship between punch force and punch displacement for both flattening mechanisms.

Figure 7 shows the relationship between punch-force and punch displacement for both the flattening mechanisms. It is observed that the punch force requirement is more when the friction is assumed to depend on both the normal loading and stretching phenomena. In the friction model some amount of force is required when straining of the asperities are assumed. In view of the above, requirement of punch force is more for the friction model involving normal loading and stretching.

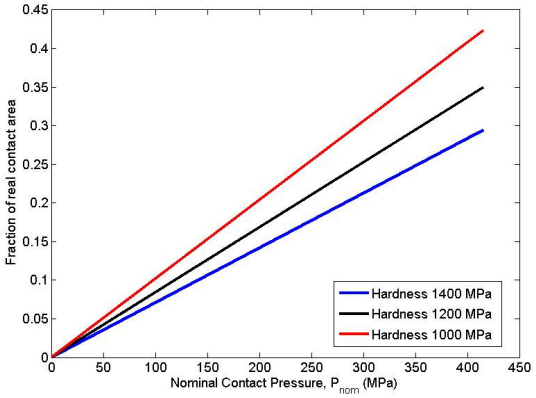

Figure 8: Dependence of fractional contact area on nominal contact pressure

Figure 8 shows the relationship between the fraction of real contact area and contact pressure ($P_{nom} = F_N / A_{nom}$) for different values of the hardness of surface asperities. It is observed that the value of fractional real contact area increases as the nominal contact pressure increases. The increase in the nominal contact pressure crushes the surface asperities giving rise to more real contact area. Further, the fractional real contact area decreases with hardness for a particular value of the nominal contact pressure.

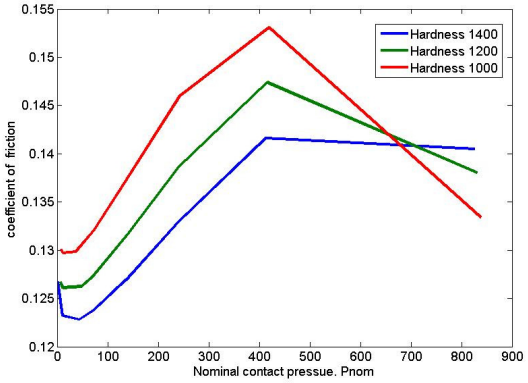

Figure 9: Dependence of coefficient of friction on nominal contact pressure

The variation of coefficient of friction with nominal contact pressure for three different hardness values is presented in Fig. 9. It is observed that the coefficient of friction first increase up to a certain value of nominal contact pressure and with the further increase in the pressure the value of the friction coefficient decreases. The value of the friction coefficient is less for higher values of the hardness. Further, it is observed that the relative decrease in the coefficient of friction is more with decrease in the hardness value when the nominal contact pressure is more than 400 MPa.

The variation of coefficient of friction with fractional real contact area for different values of the hardness is presented in Fig. 10. It is observed that friction coefficient increases with increase in the fractional real contact area for every value of hardness.

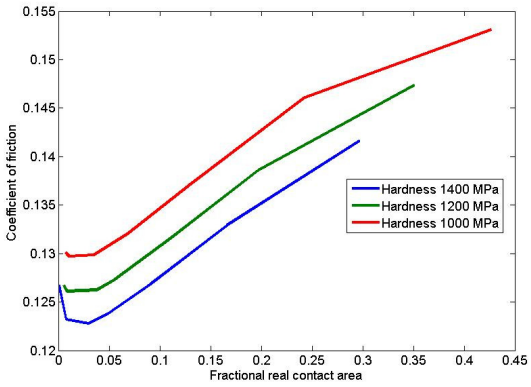

Figure 10: Dependence of coefficient of friction on fractional real contact area

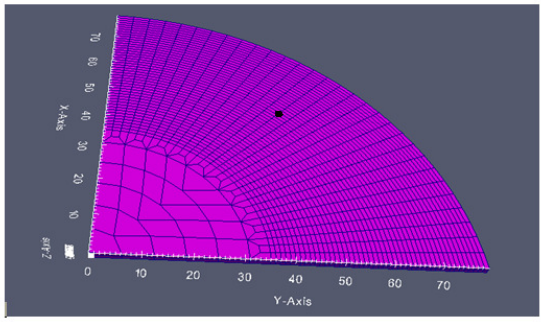

Figure 11: Location of node (under observation) in contact with die shown with black dot

Now, the trend for the coefficient of friction with punch displacement is studied. A representative node is selected for the study. As the problem is axisymmetrc any node along the circumference can be selected. Figure 11 shows the node which has been taken into consideration for studying the deep drawing parameters. The spatial coordinate of this node is (50.12, 40.34) in the undeformed configuration.

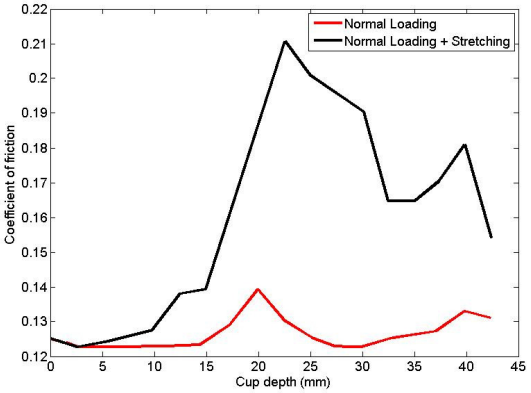

Figure 12: Variation of friction coefficient with cup depth for a node in contact with die

Figure 12 shows the variation of the friction coefficient for the representative node in contact with die for both the flattening models. The friction coefficient increases

with the puch displacemnet. Initially there is slow increase in the coefficient of friction which reaches a maximum value when the node is on the die profile radius region. It again starts decreasing before leaving its contact with the die.

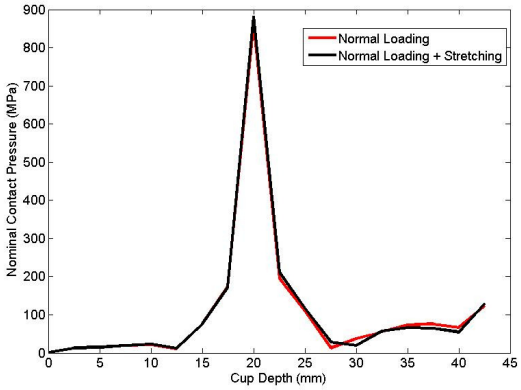

Figure 13: Variation of Nominal pressure with cup depth for a node in contact with die

Figure 13 shows the distribution of the nominal contact pressure with cup depth. The value of the nominal contact pressure is in the range of 10-20 MPa when the node remains on die. It is further observed that there is steep jump in the nominal contact pressure to the value of 850-900 MPa when the node is on the die profile radius and again it decreases to a value of 20-30 MPa. When the node is on and near to die profile radius there is a steep jump in the nominal contact pressure due to large deformation of the material and corresponding constraining forces from the geometry of the process.

4. Conclusions

A localized friction model involving flattening mechanism viz. normal loading and stretching of sheet material at microscopic level, is incorporated in an in-house deep drawing finite element code on MATLAB. A statistical approach is adapted to translate the microscopic models to a macroscopic level. It is observed that friction coefficient is dependent on both the flattening mechanisms and predicts a reasonable value of the friction coefficient at various locations along the die-sheet interface.

REFERENCES

Altan, T., Tekkaya, A.E., Sheet Metal Forming Fundamentals, *ASM International*, 2012

Bowden F.P. and Tabor D., Friction and Lubrication, *Methuen and Co. Ltd.*, 1967

Canudas de Wit, C., Olsson, H., Astrom, K.J. and Lischinsky, P., A new model for control of systems with friction. *IEEE Transactions on Automatic Control*, 1995, Vol. 40(3), pp.419–425,

Challen, J., Oxley, P., An explanation of the different regimes of friction and wear using asperity deformation models, *Wear,* 1979, Vol.53, pp. 229–243.

Cora, O.N., Friction analysis in cold forging, M.S thesis, *Middle East Technical University, Turkey*, December 2004.

Dahl, P.R., A solid friction model, *The Aerospace Corporation. Technical report*, 1968.

Ghosh, S., Li, M., Gardiner, D., A computational and experimental study of cold rolling of aluminium alloys with edge cracking, *Journal of Manufacturing Science & Engineering* 2004, Vol.126, pp. 74–82.

Hol, J., Cid Alfaro, M.V., de Rooij, M.B., Meinders, T., Advanced friction modeling for sheet metal forming, *Wear* , 2012, Vol. 286, pp. 66–78.

Jain, M.K., Iyengar, S.R.K., Jain, R.K., Numerical methods for Scientific and Engineering Computation, New Age International, Fourth Edition, 2003.

Karman, V., On the theory of rolling, *Z. angew. Math. Mech.*, 1925, Vol. 5, pp.139–41.

Liu C, Hartley P, Sturgess CEN, Rowe GW., Elastic–plastic finite element modelling of cold rolling of strip, *International Journal of Mechanical Sciences,* 1985, Vol. 27(7/8), pp. 531–41.

Orowan, E., A simple method of calculating roll pressure and power consumption in hot flat rolling, *Iron Steel Institute*., 1946, Vol.34, pp.124–46.

Saxena, RK, Studies on Deep Drawing Defects using Finite Element Method: Earing, Wrinkling and Damage, Ph,D. Thesis, IIT Kanpur, 2009.

Tan X., Friction modelling in connection with cold forming processes. *Ph.D. thesis* (IPT.024.00, MM00.15), Department of Manufacturing Engineering, *Technical University of Denmark*, 1999.

Tan X., Comparison of friction models in bulk metal forming, *Tribology International,* 2002, Vol. 35, pp.385–93.

Tan X, Bay N, Zhang W., On parameters affecting metal flow and friction in the double cup extrusion test. *Scand. J. Metall,* 1998, Vol. 27(6), pp.246–52.

Torrance, A.A., Galligan J., Liraut G., A Model of the Friction of a Smooth Hard Surface Sliding Over a Softer One , *Wear*, 1997, Vol.212, pp.213-220.

Wang, M. Y., Pelinescu, D. M., Contact force prediction and force closure analysis of a fixture rigid work piece with friction, *Journal of Manufacturing Science & Engineering,* 2003, Vol.125, pp.325–32

Wanheim, T., Bay, N., Petersen, A.S., A Theoretically Determined Model for Friction in Metal Working Processes, *Wear*, 1974, Vol.28, pp.251-258.

Wanheim T, Bay N, Petersen AS, The Average Effective Strain of Surface Asperities Deformed in Metal- Working Processes, *Wear,* 1975, Vol.34, pp.77–84.

Westeneng, J., Modelling of contact and friction in deep drawing processes, *Ph.D. Thesis, University of Twente, The Netherlands*, 2001.

Wilson, W., Sheu, S., Real area of contact and boundary friction in metal forming, *International Journal of Mechanical Science,* 1988, Vol. 30, pp. 475–489.

Yang, D.Y., Chung, W.J., Shim, H.B., Rigid-plastic finite element analysis of sheet metal forming processes with initial guess generation. *International Journal of Mechanical Science*, 1990, Vol. 32, No. 8, pp. 687-708.